Formation and Properties of [4Fe-4S] Clusters on the IscU Scaffold Protein†

Kala Chandramouli,‡ Mihaela-Carmen Unciuleac,§ Sunil Naik,|| Dennis R. Dean,*,§ Boi Hanh Huynh,*,|| and Michael K. Johnson*,‡

Department of Chemistry and Center for Metalloenzyme Studies, University of Georgia, Athens, Georgia 30602, Department of Biochemistry, Virginia Tech, Blacksburg, Virginia 24061, and Department of Physics, Emory University, Atlanta, Georgia 30322

Received December 31, 2006; Revised Manuscript Received March 11, 2007

ABSTRACT: Rapid and quantitative reductive coupling of two $[2Fe\text{-}2S]^{2+}$ clusters to form a single $[4Fe\text{-}4S]^{2+}$ cluster on the homodimeric IscU Fe−S cluster scaffold protein has been demonstrated by UV−visible absorption, Mössbauer, and resonance Raman spectroscopies, using dithionite as the electron donor. Partial reductive coupling was also observed using reduced Isc ferredoxin, which raises the possibility that Isc ferredoxin is the physiological reductant. The results suggest that reductive coupling of adjacent $[2Fe\text{-}2S]^{2+}$ clusters assembled on IscU provides a general mechanism for the final step in the biosynthesis of $[4Fe\text{-}4S]^{2+}$ clusters. The $[4Fe\text{-}4S]^{2+}$ center on IscU can be reduced to a $S = {}^1/_2[4Fe\text{-}4S]^{+}$ cluster ($g_{||} = 2.06$ and $g_{\perp} = 1.92$), but the low midpoint potential (< -570 mV) and instability of the reduced cluster argue against any physiological relevance for the reduced cluster. On exposure to O_2, the $[4Fe\text{-}4S]^{2+}$ cluster on IscU degrades via a semistable $[2Fe\text{-}2S]^{2+}$ cluster with properties analogous to those of the $[2Fe\text{-}2S]^{2+}$ center in $[2Fe\text{-}2S]^{2+}$ IscU. It is suggested that the ability of IscU to accommodate either $[2Fe\text{-}2S]^{2+}$ or $[4Fe\text{-}4S]^{2+}$ clusters in response to cellular redox status and/or oxygen levels may provide an effective way to populate appropriately cluster-loaded forms of IscU for maturation of different types of [Fe−S] proteins.

Cubane-type iron-sulfur clusters with [4Fe-4S] cores are one of the most common prosthetic groups in nature and function in numerous biological processes involving electron transport, catalysis, and regulation (*1*). However, despite major recent advances in understanding Fe−S cluster biosynthesis and evidence for similar biosynthetic machinery in both prokaryotes and eukaryotes (*2*, *3*), little is currently known concerning the mechanism of assembly of biological [4Fe-4S] clusters. The general mechanism for Fe−S cluster biosynthesis involves cysteine desulfurase-mediated assembly of a Fe−S cluster on a scaffold protein in the presence of an Fe^{2+} donor and subsequent transfer of a preformed cluster from scaffold to acceptor protein. Thus far, three distinct types of Fe−S cluster assembly machinery have been identified, termed the Isc (iron-sulfur cluster),[1] Suf (sulfur mobilization), and Nif (nitrogen fixation) systems, and each contains a cysteine desulfurase (IscS, SufS, or NifS) and one or more of three distinct types of scaffolding proteins/domains, designated as U-type, A-type, and Nfu-type. All three types of scaffolding proteins/domains have been shown to be capable of assembling and transferring both $[2Fe\text{-}2S]^{2+}$ and $[4Fe\text{-}4S]^{2+}$ clusters in vitro (*2*, *4*). The U-type scaffold, corresponding to IscU, SufU, and the N-terminus of NifU, is the best characterized and most widespread type of scaffold protein and contains three conserved cysteine residues that ligate a solvent-exposed $[2Fe\text{-}2S]^{2+}$ cluster, on the basis of mutagenesis results and structural studies of the monomeric zinc-bound forms of *Haemophilus influenzae* IscU (*5*) and *Streptococcus pyogenes* SufU (*6*).

Our previous work on *Azotobacter vinelandii* IscU indicated a homodimeric protein, and in vitro studies of the time course of IscS-mediated cluster assembly revealed sequential formation of forms of IscU containing one $[2Fe\text{-}2S]^{2+}$ cluster per dimer ($1\times[2Fe\text{-}2S]^{2+}$ IscU), two $[2Fe\text{-}2S]^{2+}$ clusters per dimer ($2\times[2Fe\text{-}2S]^{2+}$ IscU) and one $[4Fe\text{-}4S]^{2+}$ cluster per dimer ($[4Fe\text{-}4S]^{2+}$ IscU) (*7*, *8*). The last step occurred over several hours and was tentatively attributed to slow reductive coupling of two $[2Fe\text{-}2S]^{2+}$ clusters to form a $[4Fe\text{-}4S]^{2+}$ cluster at the subunit interface, although the nature and origin of the reductant was unclear. Here, analytical and spectroscopic evidence are presented for rapid and quantitative reductive coupling of two $[2Fe\text{-}2S]^{2+}$ clusters to form a single $[4Fe\text{-}4S]^{2+}$ cluster on IscU. Reductive coupling of adjacent $[2Fe\text{-}2S]^{2+}$ clusters is therefore proposed as a general mechanism for the final step in the biosynthesis of $[4Fe\text{-}4S]^{2+}$ clusters on IscU, and the Isc [2Fe-2S]ferredoxin (Fdx)[1] is shown to be a competent and physiologically relevant electron donor. The accompanying paper (*9*) demonstrates that only the [4Fe-4S]-containing form of IscU is competent for activation of *A. vinelandii* apo-aconitase, which requires a [4Fe-4S] cluster for its activity.

† This work was supported by grants from the National Institutes of Health (GM62542 to M.K.J. and GM47295 to B.H.H.) and the National Science Foundation (MCB-021138 to D.R.D.).

* To whom correspondence should be addressed: M.K.J., telephone 706-542-9378; fax 706-542-2353; e-mail johnson@chem.uga.edu; B.H.H., telephone 404-727-4295; fax 404-727-0873; e-mail vhuynh@emory.edu; D.R.D., telephone 540-231-5895; fax 540-231-7126, email deandr@vt.edu.

‡ University of Georgia.

§ Virginia Tech.

|| Emory University.

[1] Abbreviations: Isc, iron-sulfur cluster; Suf, sulfur mobilization; Nif, nitrogen fixation DTT, dithiothreitol; Fdx, ferredoxin; NHE, normal hydrogen electrode.

10.1021/bi6026659 CCC: $37.00
Published on Web 05/17/2007

MATERIALS AND METHODS

Purification and Preparation of Protein Samples. All of the chemicals were purchased from Sigma-Aldrich or Fisher, unless otherwise stated. Anaerobic experiments were performed under an argon atmosphere (<1 ppm O_2) in a Vacuum Atmospheres glovebox. *A. vinelandii* IscU, IscS, and IscFdx were heterologously produced in *Escherichia coli* and purified as previously described (*7*, *10*, *11*). $2\times[2Fe\text{-}2S]^{2+}$ and $[4Fe\text{-}4S]^{2+}$ forms of homodimeric IscU were prepared under strictly anaerobic conditions by IscS-mediated cluster assembly in the presence of Fe^{2+} and L-cysteine followed by purification using an 8 mL MonoQ column (GE Healthcare), as described previously (*8*). Samples of IscU and IscFdx were concentrated via ultrafiltration prior to spectroscopic studies and were in 100 mM Tris-HCl buffer, pH 7.4, with 1 mM dithiothreitol (DTT). Samples for Mössbauer spectroscopy were prepared using ^{57}Fe-enriched ferrous ammonium sulfate (>95% enrichment). The Fe−S cluster concentrations of the *A. vinelandii* IscU and IscFdx samples used in this work were based on experimentally determined extinction coefficients (as assessed by Fe and protein determinations) and were in excellent agreement with the published values ($\epsilon_{456} = 9.2$ mM^{-1} cm^{-1} for $[2Fe\text{-}2S]^{2+}$ clusters on IscU (*8*), $\epsilon_{390} = 14.8$ mM^{-1} cm^{-1} for $[4Fe\text{-}4S]^{2+}$ clusters on IscU (*8*), and $\epsilon_{458} = 7.1$ mM^{-1} cm^{-1} for IscFdx (*11*)). Stock sodium dithionite solutions were prepared under strictly anaerobic conditions in 100 mM Tris-HCl buffer, pH 7.4, with 1 mM DTT and calibrated by titration against oxidized benzyl viologen ($\epsilon_{599} = 9.3$ mM^{-1} cm^{-1} for reduced benzyl viologen) (*12*). Reduced IscFdx was prepared under strictly anaerobic conditions by addition of a 20-fold excess of sodium dithionite followed by repurification using a 10 mL HiTrap desalting column (GE Healthcare) to remove excess dithionite. Complete removal of dithionite from reduced IscFdx ($E_m = -344$ mV at pH 7) was confirmed on the basis of the inability to effect significant reduction of methyl viologen ($E_m = -450$ mV at pH 7). Photoreduction was carried out under strictly anaerobic conditions at 0 °C using 10 mM oxalate as the electron donor, 15 μM deazariboflavin, and a Xe-arc lamp as the light source.

Analytical and Spectroscopic Methods. Protein concentrations were determined by DC protein assay (Bio-Rad), using BSA as a standard. Iron concentrations were determined colorimetrically using bathophenanthroline under reducing conditions after digestion of the protein in 0.8% $KMnO_4$/0.2 M HCl. UV-visible absorption spectra were recorded under anaerobic conditions in septum-sealed 1 mm cuvettes, using a Shimadzu 3101PC scanning spectrophotometer fitted with a TCC-260 temperature controller. Molar extinction coefficients are expressed per IscU monomer. Resonance Raman spectra were recorded with a 457.9 nm excitation from a Coherent Innova 10 W argon ion laser incident on droplets of frozen protein solutions at 17 K, using an Instruments SA Ramanor U1000 scanning spectrometer fitted with a cooled RCA 31034 photomultiplier tube. X-band (~9.6 GHz) EPR spectra were recorded on a Bruker ESP300E spectrometer equipped with an ER-4116 dual-mode cavity and an Oxford instruments ESR-9 flow cryostat. Spin quantitations were carried out under nonsaturating conditions by double integration and calibrated against a 1 mM CuEDTA standard. Mössbauer spectra in the presence of weak and strong applied magnetic fields were recorded using the previously described instrumentation (*13*). Analyses of the Mössbauer data were performed with the program WMOSS (WEB Research). The zero velocity of the spectra refers to the centroid of a room-temperature spectrum of a metallic Fe foil.

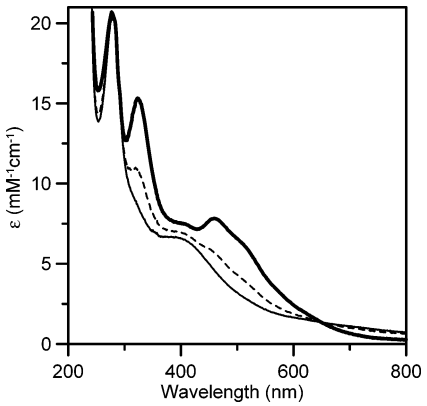

FIGURE 1: Reductive coupling of $[2Fe\text{-}2S]^{2+}$ clusters on IscU monitored by UV−visible absorption spectroscopy. UV−visible absorption spectra of $2\times[2^{57}Fe\text{-}2S]^{2+}$ IscU as prepared (thick line), reduced with 0.66 (broken line), and 1.11 (thin line) reducing equivalents of dithionite per IscU $[2Fe\text{-}2S]^{2+}$ cluster. Molar extinction coefficients are based on the concentration of IscU monomer as determined by protein assays.

RESULTS

Formation of $[4Fe\text{-}4S]^{2+}$ Clusters on IscU Via Reductive Coupling of Two $[2Fe\text{-}2S]^{2+}$ Clusters. The $2\times[2Fe\text{-}2S]^{2+}$ form of *A. vinelandii* IscU was prepared as previously described (*8*). The sample used in this study contained 1.7 $[2^{57}Fe\text{-}2S]^{2+}$ clusters per homodimer, on the basis of the published extinction coefficient as well as Fe and protein determinations and had an A_{456}/A_{280} ratio of 0.40 (compared to $A_{456}/A_{280} = 0.44$ for samples containing 2.0 $[2Fe\text{-}2S]^{2+}$ clusters per homodimer (*8*)). UV−visible absorption spectra recorded before and immediately after strictly anaerobic reduction with 0.66 and 1.11 reducing equivalents per $[2Fe\text{-}2S]^{2+}$ cluster using a freshly prepared and standardized dithionite solution are shown in Figure 1. The absorption changes occur immediately on addition of dithionite. On the basis of previous absorption studies of cluster-bound forms of IscU (*8*), the absorption spectra are indicative of near-complete reductive coupling of two $[2Fe\text{-}2S]^{2+}$ clusters to yield one $[4Fe\text{-}4S]^{2+}$ cluster after the addition of 1.1 reducing equivalents.

Parallel Mössbauer studies using the same IscU samples confirm $2\times[2Fe\text{-}2S]^{2+}$ to $[4Fe\text{-}4S]^{2+}$ reductive coupling by virtue of the distinct isomer shifts (δ) and quadrupole splittings (ΔE_Q) observed for IscU-bound $[2Fe\text{-}2S]^{2+}$ and $[4Fe\text{-}4S]^{2+}$ clusters (*8*) (Figure 2). Moreover, the Mössbauer data provide quantitative assessment of the fate of $[2Fe\text{-}2S]^{2+}$ clusters during reduction. Table 1 lists the Mössbauer parameters for $[2Fe\text{-}2S]^{2+}$, $[4Fe\text{-}4S]^{2+}$, and Fe^{2+} components. Table 2 summarizes the observed composition, compares the number of reducing equivalents added with that required to obtain the observed composition, and predicts the percent composition and number of reducing equivalents required for complete reduction of an IscU sample containing 1.7-$[2Fe\text{-}2S]^{2+}$ clusters per homodimer, on the basis of the

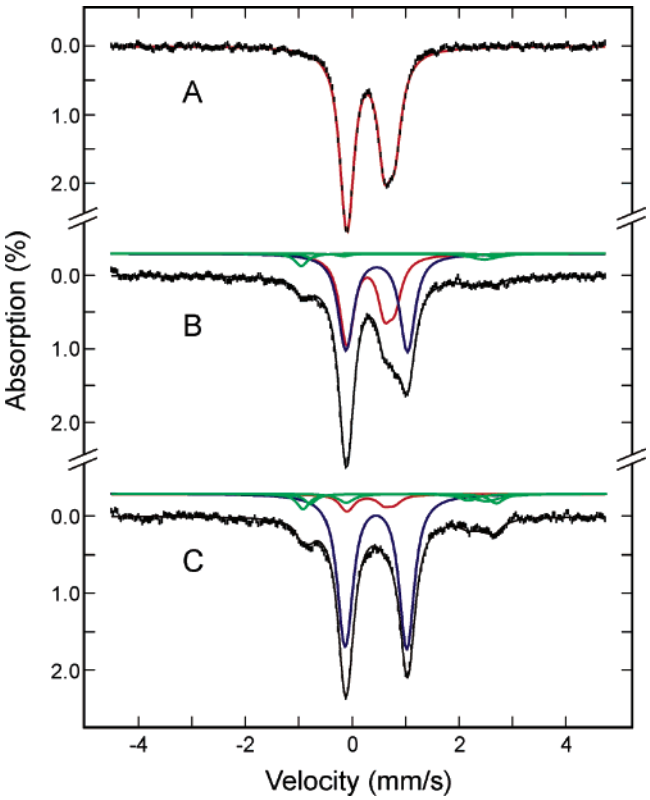

FIGURE 2: Reductive coupling of $[2Fe\text{-}2S]^{2+}$ clusters on IscU monitored by Mössbauer spectroscopy. Mössbauer spectra (4.2 K; 50 mT applied field parallel to γ radiation) of $2\times[2^{57}Fe\text{-}2S]^{2+}$ IscU as prepared (A), and reduced with 0.66 (B), and 1.11 (C) reducing equivalents of dithionite per IscU $[2Fe\text{-}2S]^{2+}$ cluster: red, IscU $[2Fe\text{-}2S]^{2+}$ clusters; blue, IscU $[4Fe\text{-}4S]^{2+}$ clusters; green, Fe^{2+} species; black, composite simulations including $[2Fe\text{-}2S]^{2+}$ and $[4Fe\text{-}4S]^{2+}$ clusters, and Fe^{2+} species formed during reduction. The samples are the same as those used in Figure 1, and the percent composition and parameters used for simulating the spectra are listed in Tables 1 and 2. Fe^{2+} species that were present prior to reduction, amounting to 5% of the total absorption, have been subtracted from each spectrum.

Table 1: Mössbauer Parameters for the Fe Species Detected in the $2\times[2Fe\text{-}2S]^{2+}$ to $[4Fe\text{-}4S]^{2+}$ IscU Reductive Coupling Experiments Shown in Figures 2 and 3

Fe species[a]	δ (mm/s)	ΔE_Q (mm/s)
$[2Fe\text{-}2S]^{2+}$		
site 1	0.27	0.66
site 2	0.32	0.94
$[4Fe\text{-}4S]^{2+}$		
site 1	0.46	1.07
site 2	0.45	1.23
Fe^{2+}_a	1.25	2.81
Fe^{2+}_b	0.78	3.42
Fe^{2+}_c	0.70	2.95

[a] A minimum of three Fe^{2+} components of various ratios is required to reproduce the ferrous contributions in spectra shown in Figures 2 and 3.

assumption that reduction of $1\times[2Fe\text{-}2S]^{2+}$ IscU is a two-electron process resulting in irreversible degradation to yield two Fe^{2+} ions, whereas reduction of $2\times[2Fe\text{-}2S]^{2+}$ IscU results in reductive coupling and the formation of $[4Fe\text{-}4S]^{2+}$ IscU in a process that requires one electron per $[2Fe\text{-}2S]^{2+}$ cluster. On addition of 0.66 reducing equivalents, 49% of the $[2Fe\text{-}2S]^{2+}$ clusters have been converted into $[4Fe\text{-}4S]^{2+}$ clusters via one-electron reduction and reductive coupling and 9% have been converted into Fe^{2+} species as a result of two-electron reduction and cluster degradation, which in total requires 0.67 reducing equivalents. On addition of 1.10 reducing equivalents, 77% of the $[2Fe\text{-}2S]^{2+}$ clusters have been converted into $[4Fe\text{-}4S]^{2+}$ clusters via one-electron reduction and reductive coupling and 15% have been converted into Fe^{2+} species as a result of two-electron reduction and cluster degradation, which in total requires 1.07 reducing equivalents. The agreement between the Mössbauer data and the number of reducing equivalents added is excellent and clearly demonstrates that dithionite reduction results in rapid reductive coupling to yield $[4Fe\text{-}4S]^{2+}$ clusters in IscU containing two $[2Fe\text{-}2S]^{2+}$ clusters per homodimer and cluster degradation in IscU containing one $[2Fe\text{-}2S]^{2+}$ cluster per homodimer.

Reductive Coupling Mediated by Reduced Isc Ferredoxin. Mössbauer spectroscopy was also used to determine if reduced IscFdx is a competent electron donor for $2\times[2Fe\text{-}2S]^{2+}$ to $[4Fe\text{-}4S]^{2+}$ reductive coupling on IscU. The $[2Fe\text{-}2S]^{2+,+}$ cluster on *A. vinelandii* IscFdx (FdIV) is stable during repeated redox cycling (*11*). Hence, Mössbauer studies offer a distinct advantage over absorption studies by facilitating selective monitoring of the fate of the [2Fe-2S] clusters on $2\times[2^{57}Fe\text{-}2S]$ IscU in samples mixed with reduced $[2^{56}Fe\text{-}2S]^{+}$ IscFdx. Analytical data indicated that the sample of $2\times[2^{57}Fe\text{-}2S]]^{2+}$ IscU used in these studies contained 1.5 $[2^{57}Fe\text{-}2S]^{2+}$ clusters per homodimer and had an A_{456}/A_{280} ratio of 0.37. Mössbauer spectra recorded before and after reduction with 1.06 equiv of reduced IscFdx and with 1.28 reducing equivalents of dithionite are shown in Figure 3. Table 2 provides the observed percent composition data for $[2Fe\text{-}2S]^{2+}$, $[4Fe\text{-}4S]^{2+}$, and Fe^{2+} components along with the number of reducing equivalents required to achieve this composition and the theoretical percent composition data assuming complete reductive coupling of $2\times[2Fe\text{-}2S]^{2+}$ IscU and complete reductive degradation of $1\times[2Fe\text{-}2S]^{2+}$ IscU.

The results demonstrate that reduced IscFdx is capable of reducing $[2Fe\text{-}2S]^{2+}$ clusters on IscU and thereby facilitates reductive coupling to yield $[4Fe\text{-}4S]^{2+}$ clusters or degradation to yield Fe^{2+} ions. However, in contrast to the near-quantitative reduction that is observed with dithionite, stoichiometric reduced IscFdx provides only 50% of a reducing equivalent and reductively couples $[2Fe\text{-}2S]^{2+}$ clusters to form $[4Fe\text{-}4S]^{2+}$ clusters in an amount (28%) that is approximately half of that (59%) formed with dithionite (Table 2). A 3-fold stoichiometric excess of reduced IscFdx was found to supply 73% of a reducing equivalent on the basis of quantitation of Mössbauer data (Table 2). However, the additional reducing equivalents appear to be channeled into reductive degradation of $[2Fe\text{-}2S]^{2+}$ clusters rather than reductive coupling.[2] The observation of partial reductive coupling with samples treated with stoichiometric and a

[2] This is likely to a be a consequence of a decrease in the proportion of IscU dimers containing two $[2Fe\text{-}2S]^{2+}$ clusters compared to the samples shown in Figure 3, as a result of an additional freeze-thaw cycle. The Mössbauer sample corresponding to Figure 3A was used to prepare the sample with a 3-fold excess of reduced IscFdx and consequently underwent an additional freeze-thaw cycle. On the basis of absorption studies, $2\times[2Fe\text{-}2S]^{2+}$-IscU loses 10−15% of its cluster content for each freeze-thaw cycle. Consequently, the percentage of $2\times[2Fe\text{-}2S]^{2+}$ to $[4Fe\text{-}4S]^{2+}$ cluster conversion is likely to have increased for a 3-fold excess of reduced IscFdx compared to stoichiometrically reduced IscFdx.

Table 2: Summary of Theoretical and Observed Results for Reductive Coupling Experiments with 2×[2Fe-2S]$^{2+}$ IscU Samples

	IscU sample	percent composition[a]			reducing equiv. per IscU [2Fe-2S]$^{2+}$ cluster		
theoretical/observed	[2Fe-2S]$^{2+}$/dimer	Fe^{2+}	[4Fe-4S]$^{2+}$	[2Fe-2S]$^{2+}$	required[a]	added (DT)	added (Fdx)
dithionite-mediated reductive coupling experiments (Figure 2)							
theoretical	1.7	17.6	82.4	0	1.17		
observed	1.7	9	49	42	0.67	0.66	
observed	1.7	15	77	8	1.07	1.1	
ferredoxin-mediated reductive coupling experiments (Figure 3)							
theoretical	1.5	33.3	66.7	0	1.33		
observed	1.5	28	59	5	1.15	1.28	
observed	1.5	11	28	61	0.50		1.06
observed	1.5	22.4	28.2	49.3	0.73		3.23

[a] As determined by analysis of Mössbauer spectra. Mössbauer parameters for the [2Fe-2S]$^{2+}$, [4Fe-4S]$^{2+}$, and Fe^{2+} species are given in Table 1.

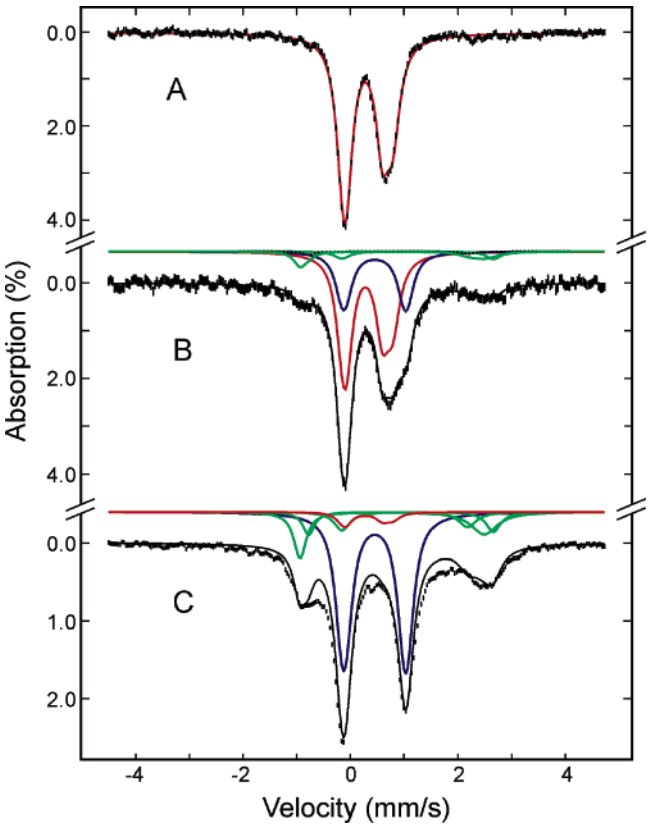

FIGURE 3: Ferredoxin-mediated reductive coupling of [2Fe-2S]$^{2+}$ clusters on IscU monitored by Mössbauer spectroscopy. Mössbauer spectra (4.2 K; 50 mT applied field parallel to γ radiation) of 2×-[2^{57}Fe-2S]$^{2+}$ IscU as prepared (A), after reduction with 1.06 reducing equivalents of reduced [2^{56}Fe-2S]$^{+}$ Fdx per IscU [2Fe-2S]$^{2+}$ cluster (B), and after reduction with 1.28 reducing equivalents of dithionite per IscU [2Fe-2S]$^{2+}$ cluster (C): red, IscU [2Fe-2S]$^{2+}$ clusters; blue, IscU [4Fe-4S]$^{2+}$ clusters; green, Fe^{2+} species; black, composite simulations including [4Fe-4S]$^{2+}$, [2Fe-2S]$^{2+}$, and Fe^{2+} species. The percent composition and parameters used for simulating the spectra are listed in Tables 1 and 2.

3-fold excess of reduced IscFdx implies that the redox potential of the [2Fe-2S]$^{2+,+}$ cluster on IscFdx ($E_m = -344$ mV) is similar to the apparent potential of the reductive coupling process. The term apparent potential is used because the reductive coupling process does not appear to be an electrochemically reversible process, see below. Hence, the Nernst equation, which predicts 50 and 75% reduction of the oxidized component if the reduced and oxidized forms of two isopotential redox centers are mixed in 1:1 and 3:1 ratios, respectively, does not strictly apply. Nevertheless, the results demonstrate that the redox potential of IscFdx is

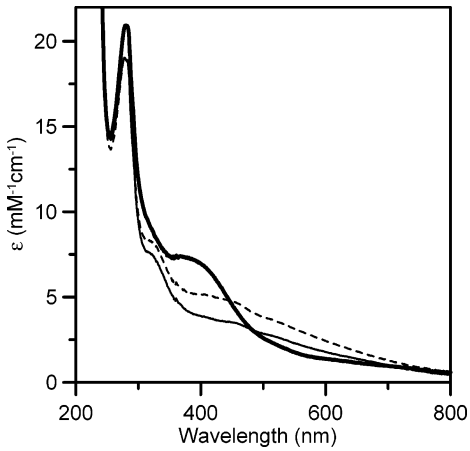

FIGURE 4: Oxygen-induced [4Fe-4S]-to-[2Fe-2S] cluster conversion on IscU monitored by UV−visible absorption spectroscopy. UV−visible absorption spectra of [4Fe-4S]$^{2+}$ IscU as prepared (thick line) and after exposure to air for 2 min (broken line) and 10 min (thin line). Molar extinction coefficients are based on the concentration of IscU monomer as determined by protein assays

poised for mediating partial formation of [4Fe-4S]$^{2+}$ clusters on IscU via the reductive coupling of two [2Fe-2S]$^{2+}$ clusters.

O_2-Induced [4Fe-4S]$^{2+}$ to [2Fe-2S]$^{2+}$ Cluster Conversion on IscU. Oxidative [4Fe-4S]$^{2+}$ to [2Fe-2S]$^{2+}$ cluster conversion was not observed on treating [4Fe-4S]$^{2+}$ IscU with oxidized IscFdx, thionine ($E_m \approx 0$ mV vs NHE) or ferricyanide ($E_m \approx 440$ mV vs NHE). Mössbauer studies indicated that the [4^{57}Fe-4S]$^{2+}$ cluster on IscU was unchanged on addition of stoichiometric oxidized [2^{56}Fe-2S]$^{2+}$ Fdx (data not shown), and UV−visible absorption studies indicated no change in the [4Fe-4S]$^{2+}$ chromophore on addition of up to a 30-fold excess of oxidized thionine. These results indicate that reductive coupling is not an electrochemically reversible process. UV−visible absorption, EPR, and resonance Raman studies in the presence of a 1-to-6-fold excess of ferricyanide showed cluster degradation with no evidence for intermediate species containing [2Fe-2S]$^{2+}$ or [3Fe-4S]$^{+}$ clusters (data not shown). However, oxidative [4Fe-4S]$^{2+}$ to [2Fe-2S]$^{2+}$ cluster conversion was apparent on exposing [4Fe-4S]$^{2+}$ IscU to limited or excess O_2 and monitoring changes in the cluster composition via UV−visible absorption and resonance Raman and Mössbauer spectroscopies (Figures 4−6, respectively).

The changes in the UV−visible absorption spectrum on exposure to air, see Figure 4, are characteristic of oxidative degradation of the [4Fe-4S]$^{2+}$ cluster via a [2Fe-2S]$^{2+}$ cluster intermediate. More definitive evidence for O_2-induced [4Fe-

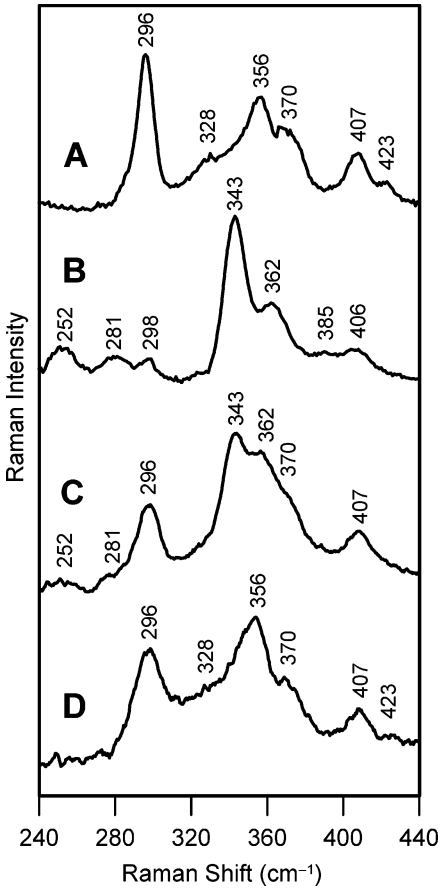

FIGURE 5: Oxygen-induced [4Fe-4S]-to-[2Fe-2S] cluster conversion on IscU monitored by resonance Raman spectroscopy. Resonance Raman spectra of 2×[2Fe-2S]$^{2+}$ IscU (A), [4Fe-4S]$^{2+}$ IscU (B), [4Fe-4S]$^{2+}$ IscU after exposure to 100 ppm O_2 for 1 min (C), and [4Fe-4S]$^{2+}$ IscU after exposure to air for 1 min (D). The sample was concentrated to ~3.5 mM prior to freezing a 17 μL droplet on the cold finger of a Displex unit at 16 K. Spectra were recorded using 457.9 nm excitation with 100 mW of laser power at the sample. Each spectrum is the sum of 100 scans, with each scan involving photon counting for 1 s at 0.5 cm^{-1} increments, with 6 cm^{-1} resolution.

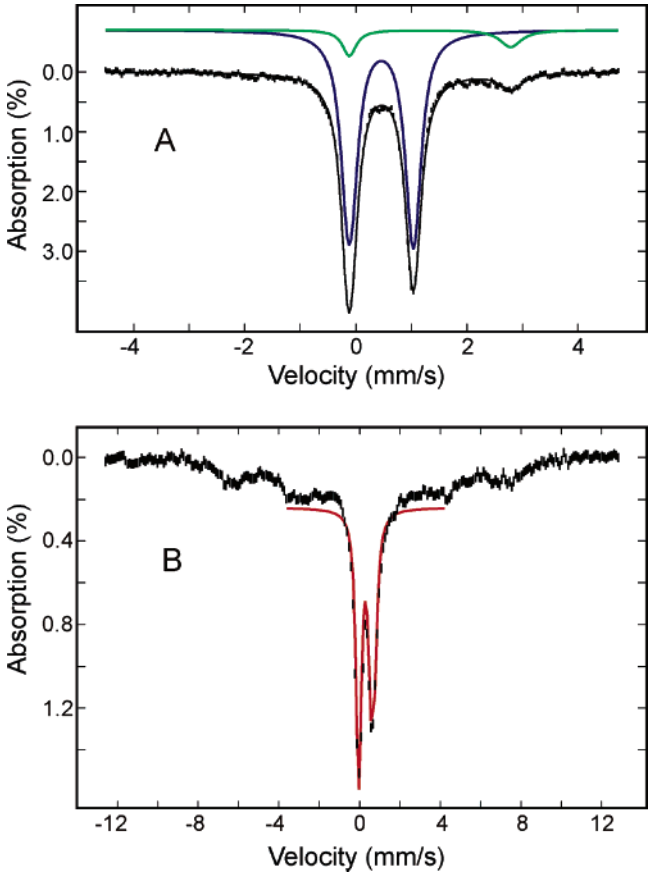

FIGURE 6: Oxygen-induced [4Fe-4S]-to-[2Fe-2S] cluster conversion on IscU monitored by Mössbauer spectroscopy. Mössbauer spectra (4.2 K; 50 mT applied field parallel to γ-radiation) of [^{57}Fe-4S]$^{2+}$ IscU as prepared (A), and after thawing the sample and exposing it to air for 15 min in the Mössbauer cuvette (B). The black line shown in A is the composite simulation including [4Fe-4S]$^{2+}$ cluster (blue line, parameters listed in Table 1) and Fe^{2+} (green line, δ = 1.31 mm/s and ΔE_Q = 2.88 mm/s) components. The red line shown in B is the simulated spectrum of a [2Fe-2S]$^{2+}$ cluster assuming two equal-intensity quadrupole doublets with the following parameters: δ (*1*) = 0.27 mm/s, ΔE_Q (*1*) = 0.56 mm/s, δ (*2*) = 0.32 mm/s, and ΔE_Q (*2*) = 0.84 mm/s. The simulated spectrum is offset from zero absorption for comparison with the central region of the experimental spectrum. Percent compositions of individual components are given in the text.

4S]$^{2+}$ to [2Fe-2S]$^{2+}$ cluster conversion was provided by resonance Raman spectroscopy. The [2Fe-2S]$^{2+}$ and [4Fe-4S]$^{2+}$ forms of IscU have distinctive resonance Raman spectra in the Fe−S stretching region, and the spectra shown in Figure 5 are in excellent agreement with previously published and assigned spectra (*7*, *8*). Resonance Raman spectra recorded after exposure of [4Fe-4S]$^{2+}$ IscU to trace amounts of O_2 and exposure to air demonstrate the progressive increase in bands associated with [2Fe-2S]$^{2+}$ clusters, at the expense of bands associated with [4Fe-4S]$^{2+}$ clusters. The close similarity in vibrational frequencies indicates that the [2Fe-2S]$^{2+}$ cluster formed via O_2 treatment of [4Fe-4S]$^{2+}$ IscU is structurally analogous to those in pristine samples of [2Fe-2S]$^{2+}$ IscU, although the increased bandwidths indicate some heterogeneity.

Mössbauer spectra confirm the UV−visible absorption and resonance Raman results and provide quantitation of the cluster conversion, see Figure 6. The Mössbauer spectrum of the [4Fe-4S]$^{2+}$ IscU sample (Figure 6A) used in these studies indicates that 90% of the Fe is present as [4Fe-4S]$^{2+}$ clusters and 10% is present as Fe^{2+} species. After thawing and exposure to air for 15 min, 32% of the Fe is present as [2Fe-2S]$^{2+}$ clusters (solid line in Figure 6B) with parameters (caption of Figure 6) similar to those of [2Fe-2S]$^{2+}$ IscU, with the remainder in the form of high-spin Fe^{3+} species that gives rise to a broad underlying signal (Figure 6B). The latter is consistent with the established lability of the [2Fe-2S]$^{2+}$ clusters on IscU upon exposure to air (*8*). Nevertheless, the spectroscopic results clearly demonstrate that [2Fe-2S]$^{2+}$ clusters similar to those present in [2Fe-2S]$^{2+}$ IscU are formed on exposure of [4Fe-4S]$^{2+}$ IscU to O_2. Overall, the spectroscopic results indicate that formation of the [4Fe-4S]$^{2+}$ cluster on IscU by reductive coupling of two [2Fe-2S]$^{2+}$ is at least partially reversed using O_2 as the electron acceptor, to yield a form of IscU with properties and cluster stoichiometry similar to those of the most stable form of IscU containing one [2Fe-2S]$^{2+}$ cluster per dimer.

Redox Properties of [4Fe-4S]$^{2+}$ IscU. The ability of excess dithionite to effect reduction of the [4Fe-4S]$^{2+}$ cluster on IscU was investigated using a combination of UV−visible absorption, EPR, and Mössbauer spectroscopies. Partial

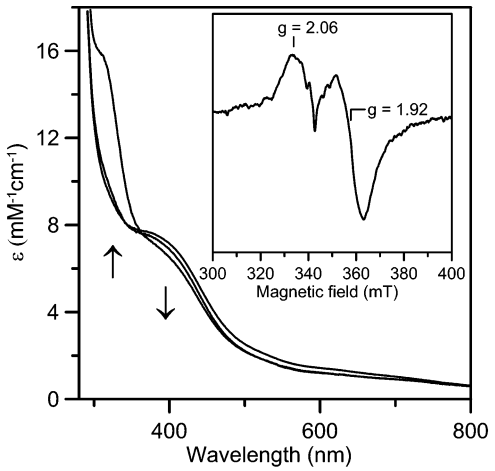

FIGURE 7: Dithionite reduction of $[4Fe\text{-}4S]^{2+}$ IscU monitored by UV−visible absorption and EPR spectroscopies. UV−visible absorption spectra of $[4^{57}Fe\text{-}4S]^{2+}$ IscU as prepared and after anaerobic addition of 3 and 7 reducing equivalents of dithionite per $[4Fe\text{-}4S]^{2+}$ cluster. Spectra are corrected for dilutions caused by the addition of dithionite, and the arrows indicate the direction of change in absorption with increasing addition of dithionite. The inset shows the EPR spectrum of the sample treated with 7 reducing equivalents recorded at 9.6 GHz and 14 K with microwave power of 10 mW and a modulation amplitude of 0.63 mT. Molar extinction coefficients are based on the concentration of IscU monomer as determined by protein assays.

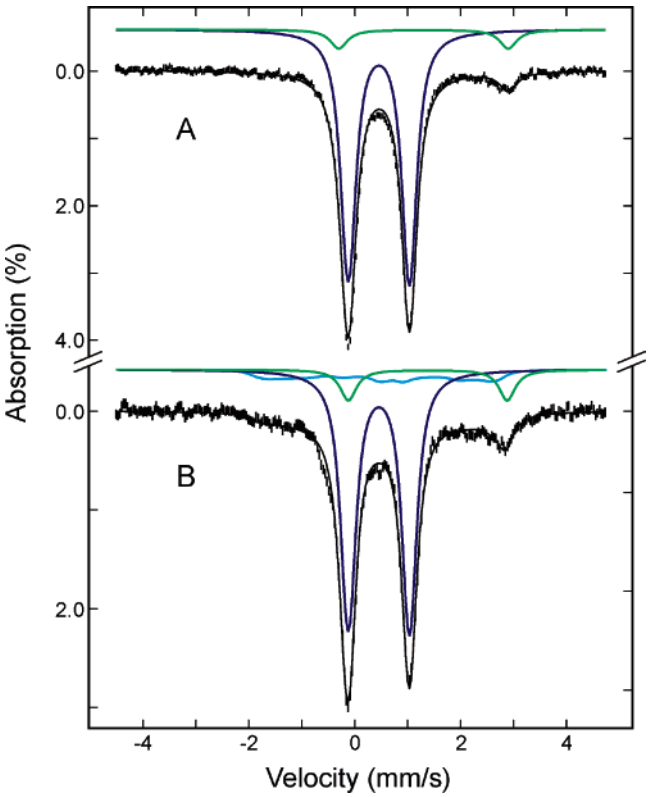

FIGURE 8: Dithionite reduction of $[4Fe\text{-}4S]^{2+}$ IscU monitored by Mössbauer spectroscopy. Mössbauer spectra (4.2 K; 50 mT applied field parallel to γ-radiation) of $[4^{57}Fe\text{-}4S]^{2+}$ IscU as prepared (A), and addition of 7 reducing equivalents of dithionite per $[4Fe\text{-}4S]^{2+}$ cluster (B): dark blue, IscU $[4Fe\text{-}4S]^{2+}$ clusters; green, Fe^{2+} species; light blue, IscU $[4Fe\text{-}4S]^{+}$ clusters; black, composite simulations including $[4Fe\text{-}4S]^{2+}$ and Fe^{2+} components (A), and $[4Fe\text{-}4S]^{2+}$, $[4Fe\text{-}4S]^{+}$, and Fe^{2+} components (B). The parameters used to simulate the $[4Fe\text{-}4S]^{2+}$ component are listed in Table 1, and the parameters used to simulate the $S = {}^1/_2$ $[4Fe\text{-}4S]^{+}$ cluster are taken from a Mössbauer study of *Bacillus stearothermophilus* ferredoxin (*14*). For the Fe^{2+} component, the parameters used are $\delta = 1.30$ mm/s and $\Delta E_Q = 3.2$ mm/s. Percent compositions of individual components are given in the text.

reduction to yield a $S = {}^1/_2$ $[4Fe\text{-}4S]^{+}$ cluster is indicated by progressive bleaching of the visible absorption band centered near 400 nm on anaerobic addition of a 3- and 7-fold stoichiometric excess of dithionite and the appearance of a fast relaxing EPR signal ($g_{\|} = 2.06$ and $g_{\perp} = 1.92$, observable only below 40 K) maximally accounting for 0.18 spins per [4Fe-4S] cluster (Figure 7). Parallel Mössbauer studies of the sample reduced with 7-fold excess of dithionite are consistent with this interpretation, see Figure 8. Prior to reduction, 90% of the Fe is in the form of $[4Fe\text{-}4S]^{2+}$ clusters and 10% is in the form of Fe^{2+} species. After reduction, 76% of the Fe is present as $[4Fe\text{-}4S]^{2+}$ clusters, 14% is present as $S = {}^1/_2[4Fe\text{-}4S]^{+}$ clusters, and 10% is present as Fe^{2+} species. Hence, the Mössbauer spectra indicate a spin concentration of 0.16 spins per [4Fe-4S] cluster, in excellent agreement with the EPR data. On the basis of the Nernst equation and the dithionite redox potential at pH 7.4 (−444 mV), 16−18% reduction of the $[4Fe\text{-}4S]^{2+}$ cluster on IscU with a 7-fold excess of dithionite indicates a redox potential of the $[4Fe\text{-}4S]^{2+,+}$ couple < -570 mV versus NHE. However, attempts to achieve a greater level of reduction by using a larger excesses of dithionite (up to 20-fold) or deazariboflavin-mediated photoreduction ($E_m \approx -600$ mV vs NHE) resulted in irreversible cluster degradation as evidence by irreversible bleaching of the visible absorption, weaker $S = {}^1/_2$ $[4Fe\text{-}4S]^{+}$ EPR signals accounting for <0.1 spins per [4Fe-4S] cluster and no evidence of low-field resonances attributable to $S = {}^3/_2$ $[4Fe\text{-}4S]^{+}$ at high microwave powers and low temperatures. The very low redox potential for the $[4Fe\text{-}4S]^{2+,+}$ couple and the instability of the $[4Fe\text{-}4S]^{+}$ clusters on IscU indicate that this is unlikely to be a physiologically relevant redox state.

DISCUSSION

U-type scaffold proteins are present in the Isc, Suf, and Nif systems for Fe−S cluster assembly and constitute the most ubiquitous and best-characterized class of Fe−S cluster scaffold proteins (*2*, *4*−*6*). In vitro studies of IscU, SufU, and NifU proteins have established that U-type scaffold proteins or domains are capable of cysteine desulfurase-mediated assembly of oxidatively and reductively labile $[2Fe\text{-}2S]^{2+}$ clusters that can be transferred intact into acceptor proteins (*7*, *15*−*18*). In contrast, the ability of U-type scaffold proteins or domains to assemble $[4Fe\text{-}4S]^{2+}$ clusters has thus far only been demonstrated for *A. vinelandii* IscU (*8*) and NifU (*4*), and the objective of this work was to provide insight into the determinants, mechanism, and significance of $[4Fe\text{-}4S]^{2+}$ cluster assembly on U-type scaffold proteins. The results reported in this manuscript provide direct evidence for rapid and quantitative formation of $[4Fe\text{-}4S]^{2+}$ clusters at the subunit interface of homodimeric *A. vinelandii* IscU via reductive coupling of two $[2Fe\text{-}2S]^{2+}$ clusters and show that IscFdx is a competent electron donor for achieving partial reductive coupling. The accompanying paper addresses significance by demonstrating that only the [4Fe-4S]-containing form of IscU is competent for the activation of *A. vinelandii* apo-aconitase.

A. vinelandii IscU is a homogeneous homodimer in solution as judged by size exclusion chromatography (*7*) and

dynamic light scattering (Dean, D. R, and Mayer, S. M., unpublished results). In contrast, structural studies of *H. influenzae* IscU (*5*) and *S. pyogenes* SufU (*6*) have revealed monomeric proteins with Zn bound at the putative solvent-exposed cluster binding sites. As discussed below, dimerization with the cluster binding sites at the subunit interface is clearly a key determinant of the ability of IscU proteins to assemble $[4Fe\text{-}4S]^{2+}$ clusters.

IscS-mediated cluster assembly on apo-IscU was found to be a sequential process with initial formation of a stable species containing one $[2Fe\text{-}2S]^{2+}$ cluster per dimer, progressing through a form containing two $[2Fe\text{-}2S]^{2+}$ clusters per dimer, and ending with slow conversion to a form containing one $[4Fe\text{-}4S]^{2+}$ cluster per dimer over a period of several hours (*7*, *8*). By using the combination of UV−visible absorption and Mössbauer spectroscopy, the present work demonstrates that conversion of $2\times[2Fe\text{-}2S]^{2+}$ IscU to $[4Fe\text{-}4S]^{2+}$ IscU is a two-electron process that occurs quantitatively and immediately on addition of one reducing equivalent of dithionite per $[2Fe\text{-}2S]^{2+}$ cluster. Coupled with the analytical evidence for one $[4Fe\text{-}4S]^{2+}$ cluster per IscU dimer (*8*), this result indicates one-electron reduction of spatially proximal $[2Fe\text{-}2S]^{2+}$ clusters at the subunit interface followed by rapid coupling to yield a subunit bridging $[4Fe\text{-}4S]^{2+}$ cluster. The observation of reductive degradation of $[2Fe\text{-}2S]^{2+}$ clusters lacking a partner cluster within the homodimeric complex is consistent with established reductive lability of $[2Fe\text{-}2S]^{2+}$ clusters on $1\times[2Fe\text{-}2S]^{2+}$ IscU (*7*, *8*) and provides additional support for this interpretation.

These results prompted evaluation of the possibility that reduced Isc-specific $[2Fe\text{-}2S]^{2+,+}$ Fdx ($E_m = -344$ mV) could be the physiological one-electron donor responsible for promoting rapid $[4Fe\text{-}4S]^{2+}$ cluster formation on IscU via reductive coupling of $[2Fe\text{-}2S]^{2+}$ clusters. IscFdx is encoded by the *isc* operon in many prokaryotic organisms, including *A. vinelandii*, and plays a key role in eukaryotic Fe−S cluster assembly, but the physiological redox role has yet to be identified (*2*, *3*). The Mössbauer studies presented herein demonstrate that reduced IscFdx is a competent reductant for mediating partial $[4Fe\text{-}4S]^{2+}$ formation via reductive coupling of $[2Fe\text{-}2S]^{2+}$ clusters on IscU. It is tempting to speculate that the IscFdx redox potential is poised to induce partial reductive coupling in order to make IscU a more versatile and environmentally responsive scaffold protein. Maintaining a balance between $[2Fe\text{-}2S]^{2+}$ and $[4Fe\text{-}4S]^{2+}$ cluster-bound forms of IscU renders IscU capable of providing clusters for the maturation of both [2Fe-2S]- and [4Fe-4S]-containing proteins. In addition, it would provide a sensitive mechanism for controlling the balance between $[2Fe\text{-}2S]^{2+}$ and $[4Fe\text{-}4S]^{2+}$ cluster-bound forms of IscU in response to changes in the cellular redox potential.

Although reductive coupling of two $[2Fe\text{-}2S]^{2+}$ clusters to yield $[4Fe\text{-}4S]^{2+}$ IscU does not appear to be a reversible redox process, spectroscopic results clearly demonstrate that O_2 exposure results in $[4Fe\text{-}4S]^{2+}$ to $[2Fe\text{-}2S]^{2+}$ cluster conversion. Similar O_2-induced $[4Fe\text{-}4S]^{2+}$ to $[2Fe\text{-}2S]^{2+}$ cluster conversions have been observed in the fumarate and nitrate reduction (FNR) regulatory protein and in radical-SAM enzymes (*1*, *19*−*21*). The most recent evidence indicates that the cluster conversion in FNR occurs via one-electron oxidation to form superoxide and an unstable $[4Fe\text{-}4S]^{3+}$ cluster that immediately releases an Fe^{2+} ion to form a transient $[3Fe\text{-}4S]^{+}$ cluster (*22*). The $[3Fe\text{-}4S]^{+}$ cluster subsequently degrades with the loss of Fe^{3+} and two S^{2-} ions to form a $[2Fe\text{-}2S]^{2+}$ cluster. Transient $[3Fe\text{-}4S]^{+}$ clusters have also been observed in the O_2-induced $[4Fe\text{-}4S]^{2+}$ to $[2Fe\text{-}2S]^{2+}$ cluster degradation in many radical-SAM enzymes (*21*). Although there is as yet no spectroscopic evidence for a transient $[3Fe\text{-}4S]^{+}$ cluster intermediate in O_2-induced $[4Fe\text{-}4S]^{2+}$ to $[2Fe\text{-}2S]^{2+}$ cluster conversion on IscU, a similar mechanism currently represents our best working hypothesis. The spectroscopic studies presented in this work indicate that the product of this O_2-induced cluster conversion is similar to the most-stable cluster-bound form of IscU containing one $[2Fe\text{-}2S]^{2+}$ cluster per dimer (*8*), and this form of IscU has recently been shown to be catalytically competent for ATP-dependent $[2Fe\text{-}2S]^{2+}$ cluster transfer to apo-IscFdx (*18*). Taken together, these observations suggest that IscU can switch from being a [4Fe-4S]-cluster donor to a [2Fe-2S]-cluster donor in response to oxidative stress and cellular O_2 levels. Because biological $[2Fe\text{-}2S]^{2+}$ centers are generally less sensitive to degradation by reactive O_2 species than $[4Fe\text{-}4S]^{2+}$ clusters, the ability of IscU to switch to scaffolding predominantly [2Fe-2S] clusters under conditions of oxidative stress may well be physiologically relevant. Overall, the picture of IscU that emerges from these in vitro studies is therefore of a versatile scaffold protein that is capable of modulating between $[2Fe\text{-}2S]^{2+}$ and $[4Fe\text{-}4S]^{2+}$ cluster-bound forms in response to cellular redox status and oxygen levels in order to populate appropriately cluster-loaded forms of IscU for maturation of different types of [Fe−S] proteins.

The results presented in this work beg the question of how $[4Fe\text{-}4S]^{2+}$ clusters are formed, albeit very slowly over a period of several hours, during IscS-mediated cluster assembly in the absence of an exogenous one-electron reductant (*8*). The most probable explanation is that the two electrons required for reductive coupling can be provided by the formation of a disulfide between two of the cysteines released on formation of the $[4Fe\text{-}4S]^{2+}$ cluster. Precedent for this type of reaction is provided by studies of analog clusters in aprotic media. Holm and co-workers first demonstrated reductive coupling of two thiolate-ligated $[2Fe\text{-}2S]^{2+}$ clusters to yield a thiolate-ligated $[4Fe\text{-}4S]^{2+}$ cluster and a thiol disulfide in 1981 (*23*). As yet, there is no direct evidence for disulfide formation accompanying $[4Fe\text{-}4S]^{2+}$ cluster formation on IscU. However, disulfide formation and cleavage could play key roles in the assembly or release of $[4Fe\text{-}4S]^{2+}$ clusters on IscU, and experiments are in progress to evaluate this possibility.

REFERENCES

1. Johnson, M. K., and Smith, A. D. (2005) Iron-sulfur proteins, in *Encyclopedia of Inorganic Chemistry* (Crabtree, R. H., Ed.) 2nd ed., pp 2589−2619, John Wiley & Sons, Chichester, U.K.
2. Johnson, D., Dean, D. R., Smith, A. D., and Johnson, M. K. (2005) Structure, function and formation of biological iron-sulfur clusters, *Annu. Rev. Biochem. 74*, 247−281.
3. Lill, R., and Mühlenhoff, U. (2005) Iron-sulfur-protein biogenesis in eukaryotes, *Trends Biochem. Sci. 30*, 133−141.
4. Smith, A. D., Jameson, G. N. L., Dos Santos, P. C., Agar, J. N., Naik, S., Krebs, C., Frazzon, J., Dean, D. R., Huynh, B. H., and Johnson, M. K. (2005) NifS-mediated assembly of [4Fe-4S] clusters in the N- and C-terminal domains of the NifU scaffold protein, *Biochemistry 44*, 12955−12969.

5. Ramelot, T. A., Cort, J. R., Goldsmith-Fischman, S., Kornhaber, G. J., Xiao, R., Shastry, R., Acton, T. B., Honig, B., Montelione, G. T., and Kennedy, M. A. (2004) Solution NMR structure of the iron-sulfur cluster assembly protein U (IscU) with zinc bound at the active site, *J. Mol. Biol. 344*, 567−583.
6. Liu, J., Oganesyan, N., Shin, D. H., Jancarik, J., Yokota, H., Kim, R., and Kim, S.-H. (2005) Structural characterization of an iron-sulfur cluster assembly protein IscU in a zinc-bound form, *Proteins: Struct., Funct., Bioinf. 59*, 875−881.
7. Agar, J. N., Zheng, L., Cash, V. L., Dean, D. R., and Johnson, M. K. (2000) Role of the IscU protein in iron-sulfur cluster biosynthesis: IscS-mediated assembly of a [Fe_2S_2] cluster in IscU, *J. Am. Chem. Soc. 122*, 2136−2137.
8. Agar, J. N., Krebs, B., Frazzon, J., Huynh, B. H., Dean, D. R., and Johnson, M. K. (2000) IscU as a scaffold for iron-sulfur cluster biosynthesis: Sequential assembly of [2Fe-2S] and [4Fe-4S] clusters in IscU, *Biochemistry 39*, 7856−7862.
9. Unciuleac, M.-C., Chandramouli, K., Naik, S., Mayer, S., Huynh, B. H., Johnson, M. K., and Dean, D. R. (2007) In vitro activation of apo-aconitase using a [4Fe-4S] cluster-loaded form of the IscU [Fe-S] cluster scaffolding protein, *Biochemistry 46*, 6812−6821.
10. Zheng, L., Cash, V. L., Flint, D. H., and Dean, D. R. (1998) Assembly of iron-sulfur clusters. Identification of an *iscSUA-hscBA-fdx* gene cluster from *Azotobacter vinelandii*, *J. Biol. Chem. 273*, 13264−13272.
11. Jung, Y.-S., Gao-Sheridan, H. S., Christiansen, J., Dean, D. R., and Burgess, B. K. (1999) Purification and biophysical characterization of a new [2Fe-2S] ferredoxin from *Azotobacter vinelandii*, a putative [Fe-S] cluster assembly/repair protein, *J. Biol. Chem. 274*, 32402−32410.
12. Heo, J., Staples, C. R., and Ludden, P. W. (2001) Redox-dependent CO_2 reduction activity of CO dehydrogenase from Rhodospirillum rubrum, *Biochemistry 40*, 7604−7611.
13. Ravi, N., Bollinger, J. M., Huynh, B. H., Edmondson, D. E., and Stubbe, J. (1994) Mechanism of assembly of the tyrosyl radical-diiron(III) cofactor of *E. coli* ribonucleotide reductase. 1. Mössbauer characterization of the diferric radical precusor, *J. Am. Chem. Soc. 116*, 8007−8014.
14. Middleton, P., Dickson, D. P. E., Johnson, C. E., and Rush, J. D. (1978) Interpretation of the Mössbauer spectra of the four-iron ferredoxin from *Bacillus stearothermophilus*, *Eur. J. Biochem. 88*, 135−141.
15. Yuvaniyama, P., Agar, J. N., Cash, V. L., Johnson, M. K., and Dean, D. R. (2000) NifS-directed assembly of a transient [2Fe-2S] cluster within the NifU protein, *Proc. Natl. Acad. Sci. U.S.A. 97*, 599−604.
16. Wu, S.-P., Wu, G., Surerus, K. K., and Cowan, J. A. (2002) Iron-sulfur cluster biosynthesis: Kinetic analysis of [2Fe-2S] cluster transfer from holo ISU to apo Fd: Role of redox chemistry and a conserved aspartate, *Biochemistry 41*, 8876−8885.
17. Mansy, S. S., Wu, G., Surerus, K. K., and Cowan, J. A. (2002) Iron-sulfur cluster biosynthesis. Thermatoga maritima IscU is a structured iron-sulfur cluster assembly protein, *J. Biol. Chem. 277*, 21397−21404.
18. Chandramouli, K., and Johnson, M. K. (2006) HscA and HscB stimulate [2Fe-2S] cluster transfer from IscU to apoferredoxin in an ATP-dependent reaction, *Biochemistry 45*, 11087−11095.
19. Kiley, P. J., and Beinert, H. (1998) Oxygen sensing by the global regulator, FNR: The role of the iron-sulfur cluster, *FEMS Microbiol. Rev. 22*, 341−352.
20. Crack, J., Green, J., and Thomson, A. J. (2004) Mechanism of oxygen sensing by the bacterial transcriptional factor fumarate-nitrate reduction (FNR), *J. Biol. Chem. 279*, 9278−8286.
21. Cosper, M. M., Krebs, B., Hernandez, H., Jameson, G., Eidsness, M. K., Huynh, B. H., and Johnson, M. K. (2004) Characterization of the cofactor content of *Escherichia coli* biotin synthase, *Biochemistry 43*, 2007−2021.
22. Crack, J. C., Green, J., Cheeseman, M. R., Le Brun, N. E., and Thomson, A. J. (2007) Superoxide-mediated amplification of the oxygen-induced switch from [4Fe-4S] to [2Fe-2S] clusters in the transcriptional regulator FNR, *Proc. Natl. Acad. Sci. U.S.A. 104*, 2092−2097.
23. Hagen, K. S., Reynolds, J. G., and Holm, R. H. (1981) Definition of reaction sequences resulting in self-assembly of $[Fe_4S_4(SR)_4]^{2-}$ clusters from simple reactants, *J. Am. Chem. Soc. 103*, 4054−4063.

BI6026659